

Spin-dependent tunneling spectroscopy in MgO-based double-barrier magnetic tunnel junctions

G. Q. Yu, H. Kurt, J. F. Feng, K. XU, J. M. D. Coey, and X. F. Han

Citation: *Journal of Applied Physics* **111**, 07C712 (2012); doi: 10.1063/1.3677776

View online: <http://dx.doi.org/10.1063/1.3677776>

View Table of Contents: <http://scitation.aip.org/content/aip/journal/jap/111/7?ver=pdfcov>

Published by the AIP Publishing

Articles you may be interested in

[Tunneling processes in asymmetric double barrier magnetic tunnel junctions with a thin top MgO layer](#)

J. Appl. Phys. **114**, 213909 (2013); 10.1063/1.4838116

[Effects of elemental distributions on the behavior of MgO-based magnetic tunnel junctions](#)

J. Appl. Phys. **109**, 103909 (2011); 10.1063/1.3583569

[Influence of annealing on the bias voltage dependence of tunneling magnetoresistance in MgO double-barrier magnetic tunnel junctions with CoFeB electrodes](#)

Appl. Phys. Lett. **89**, 162501 (2006); 10.1063/1.2362977

[Tunneling spectroscopy in CoFeB MgO CoFeB magnetic tunnel junctions](#)

J. Appl. Phys. **99**, 08A905 (2006); 10.1063/1.2173628

[Inelastic tunneling spectroscopy of magnetic tunnel junctions based on CoFeB MgO CoFeB with Mg insertion layer](#)

J. Appl. Phys. **99**, 08T305 (2006); 10.1063/1.2162047

High-Voltage Amplifiers

- Voltage Range from $\pm 50\text{V}$ to $\pm 60\text{kV}$
- Current to 25A

Electrostatic Voltmeters

- Contacting & Non-contacting
- Sensitive to 1mV
- Measure to 20kV



ENABLING RESEARCH AND
INNOVATION IN DIELECTRICS,
ELECTROSTATICS,
MATERIALS, PLASMAS AND PIEZOS



www.trekinc.com

TREK, INC. 190 Walnut Street, Lockport, NY 14094 USA • Toll Free in USA 1-800-FOR-TREK • (t):716-438-7555 • (f):716-201-1804 • sales@trekinc.com

Spin-dependent tunneling spectroscopy in MgO-based double-barrier magnetic tunnel junctions

G. Q. Yu,^{1,2,3} H. Kurt,² J. F. Feng,² K. XU,¹ J. M. D. Coey,² and X. F. Han^{3,a)}

¹Platform for Characterization and Test, Suzhou Institute of Nano-Tech and Nano-Bionics, Chinese Academy of Sciences, Suzhou 215125, China

²CRANN and School of Physics, Trinity College, Dublin 2, Ireland

³Beijing National Laboratory for Condensed Matter Physics, Institute of Physics, Chinese Academy of Sciences, Beijing 100190, China

(Presented 2 November 2011; received 23 September 2011; accepted 17 November 2011; published online 8 March 2012)

We investigated the dynamic conductance and inelastic electron tunneling spectroscopy in MgO-based double barrier magnetic tunnel junctions with Co₅₀Fe₅₀/Co₄₀Fe₄₀B₂₀ hybrid free layers. The tunneling is coherent through the MgO (001) barriers but nonresonant, and the highest tunneling magnetoresistance reaches 260% at 2 K. Based on the detailed discussion of the tunneling mechanisms, the double-barrier junctions investigated here can be considered as two single-barrier junctions in series. © 2012 American Institute of Physics. [doi:10.1063/1.3677776]

I. INTRODUCTION

Tunneling magnetoresistance (TMR) effect in MgO-based single-barrier magnetic tunnel junctions (SMTJs) has been widely studied due to its great potential applications in magnetic random access memory (MRAM) and field sensors.^{1,2} However, the TMR ratio in SMTJs falls off quickly with increasing bias voltage,³ which limits its wider applications. In contrast to SMTJs, double barrier MTJ (DMTJ), where the voltage is divided over two single junctions, shows an improved bias dependence of TMR ratio.^{3,4} Recently, a TMR ratio of over 200% has been achieved in MgO-based DMTJs at room temperature (RT) by using Co₅₀Fe₅₀/Co₄₀Fe₄₀B₂₀ hybrid free layer.^{5,6} On the other hand, the spin-dependent resonant tunneling effect in DMTJs, which is reflected by an oscillation of the tunneling conductance, has attracted a lot of interest.^{7,8} The tunneling mechanism in DMTJs with such high TMR ratio becomes interesting.

For MTJs, the measurement of dynamic conductance (dI/dV) and the inelastic electron tunnel spectroscopy (IETS- d^2I/dV^2) has been proven to be a very powerful tool to investigate spin-dependent tunneling.^{9,10} There has been much work devoted to the dI/dV and IET spectra in MgO SMTJs.⁹⁻¹⁶ However, much less attention has been paid to MgO DMTJs. In this study, the measurement of dynamic conductance and IET spectra in MgO-based DMTJs with a Co₅₀Fe₅₀/Co₄₀Fe₄₀B₂₀ free layer was carried out using a SMTJ as a reference.

II. EXPERIMENT AND THEORETICAL METHODS

DMTJ and SMTJ stacks were grown on thermally oxidized silicon wafers with layer sequences Ta 5/Ru 30/Ta 5/ Ni₈₁Fe₁₉ 5/Ir₂₂Mn₇₈ 10/Co₉₀Fe₁₀ 2.5/Ru 0.9/Co₄₀Fe₄₀B₂₀ (CoFeB) 3/MgO 2.5/Co₅₀Fe₅₀(CoFe) 2/CoFeB t /MgO 2.5/CoFeB 3/Ru 0.9/ Co₉₀Fe₁₀ 2.5/ Ir₂₂Mn₇₈ 10/ Ni₈₁Fe₁₉ 5/Ta

5/Ru 5 and Ta 5/Ru 30/Ta 5/ Ni₈₁Fe₁₉ 5/ Ir₂₂Mn₇₈ 10/ Co₉₀Fe₁₀ 2.5/Ru 0.9/CoFeB 3/MgO 2.5/CoFeB 3/Ta 5/Ru 5 (in nm). The MgO layer was rf-sputtered from a target facing target source, whereas, the metal layers were deposited by dc-magnetron sputtering. All were grown in a high vacuum using a Shamrock cluster deposition tool at RT. The thickness of CoFeB for the combined free layer in the DMTJs is 0, 0.5, 0.8, or 1.0 nm. Junctions with size $10 \times 10 \mu\text{m}^2$ were fabricated by conventional UV lithography combined with argon ion milling and lift-off techniques. The samples were then annealed at annealing temperature (T_a) ranging from 250 to 375 °C in high vacuum for 1 h under an in-plane magnetic field of 0.8 T. The magnetotransport properties were performed in a Physical Properties Measurement System using a conventional four-point method. Dynamic conductance and IET spectra were measured at 30.79 Hz with an ac modulation voltage of 4 mV using a standard lock-in method. The details of IET spectra measurement can be found in our previous papers.⁹⁻¹¹

III. RESULTS AND DISCUSSIONS

Figure 1 shows the T_a dependences of the TMR ratios at RT for the DMTJs and SMTJ. The TMR ratios of DMTJs and SMTJ increase with increasing annealing temperature up to $T_a = 375$ °C. The maximum TMR ratio for the SMTJ reaches 297%, whereas the TMR ratio of the DMTJ with the CoFe free layer is only 160% at RT. This TMR ratio is considerably enhanced with the insertion of amorphous CoFeB between CoFe and the upper MgO layer, reaching 192% and 222% for $t_{\text{CoFeB}} = 0.5$ and 1 nm, respectively. The reason for the enhanced TMR ratio is that the amorphous CoFeB grown on polycrystalline CoFe in the free layer facilitates the growth of a higher quality upper MgO tunnel barrier, and the 2 nm thick CoFe absorbs the boron when the thin CoFeB is annealed to produce the crystallized free layer that is needed for high TMR.⁵ The TMR ratio for $t_{\text{CoFeB}} = 0.5$ nm is not as high as that for $t_{\text{CoFeB}} = 1.0$ nm, which could be due to

^{a)}Author to whom correspondence should be addressed. Electronic mail: xfhan@aphy.iphy.ac.cn.

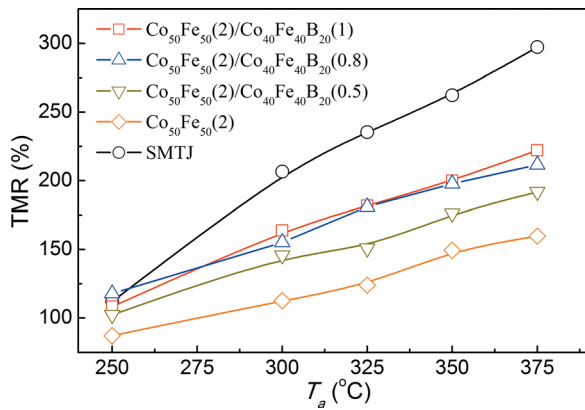


FIG. 1. (Color online) Annealing temperature (T_a) dependences of TMR ratios at room temperature for the SMTJ (Ref. 6) and the DMTJs with $t_{\text{CoFeB}} = 0$ (Ref. 6), 0.5 (Ref. 6) and 1 nm.

incomplete coverage of the CoFe by the thin CoFeB, and the subsequently grown MgO has a poor texture.

Figure 2(a) shows the temperature dependences of TMR ratio and resistance for DMTJ with $t_{\text{CoFeB}} = 1.0$ nm. The TMR ratio increases with decreasing temperature and reaches 260% at 2 K. The resistance is almost independent of temperature for the parallel configuration but increases with decreasing temperature for the antiparallel configuration, which are commonly observed features of MgO SMTJs.² Figure 2(b) shows the temperature dependence of quality factor, $Q = \text{TMR}_{\text{top}}/\text{TMR}_{\text{total}}$, where $\text{TMR}_{\text{bottom}}$ and TMR_{top} are the resistance changes in the bottom and top tunnel barriers divided by the total resistance of the DMTJ. The Q factor decreases with decreasing temperature, which reflects that the TMR contribution of top MTJ gets smaller at lower temperature. This may be due to poor antiparallel alignment between the free and top pinned layers resulting

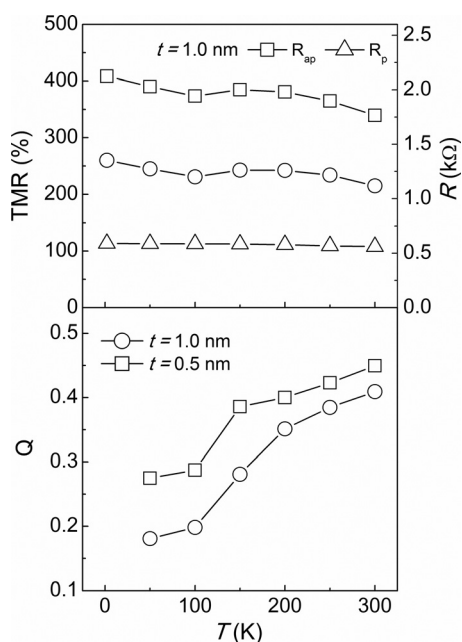


FIG. 2. (a) Temperature dependences of TMR ratio and resistances of parallel and antiparallel states for $t_{\text{CoFeB}} = 1.0$ nm. (b) Temperature dependence of Q factor for $t_{\text{CoFeB}} = 0.5$ and 1.0 nm.

from the complex changes with temperature of the exchange bias of the top pinned layer and the coercivity of the free layer.

Figure 3(a) shows the dynamic conductance of SMTJ and DMTJs with $t_{\text{CoFeB}} = 0.5$ and 1.0 nm for the parallel configuration. The dynamic conductance shows symmetric features as a function of the bias voltage for $t_{\text{CoFeB}} = 1$ nm but distinctly asymmetric features for $t_{\text{CoFeB}} = 0.5$ nm. The asymmetric bias dependence probably originates from a difference in quality between top and bottom MgO barriers.

In addition, some unambiguous features at low bias were observed in dI/dV curve for DMTJs. These detailed features were not observed in the previous work in DMTJs with thin CoFeB layer, in which the TMR is very low compared to the present samples.¹⁷ The IET spectra also shows several peaks at low bias for the parallel state, as shown in Figs. 4(a), 4(b), and 4(c), which can be identified from the features in the dI/dV curves. It is necessary to point out that the IET spectra was measured by a lock-in method, and not derived by numerical differentiation of the dI/dV curve. To understand the origin of features in the dI/dV curves and peaks in the IET spectra, we compared the results with those for a SMTJ. For the SMTJ, the bias axis is multiplied by 2, and thus it can be considered as a supposed DMTJ composed by two identical SMTJs without any interaction between them. In the dI/dV curves, the features for DMTJs are quite similar to those of the scaled SMTJ. In the IET spectra, all the positions of peaks for DMTJs correspond well to those of the scaled SMTJ, labeled by dashed lines. In addition, there are double minima of the conductance in DMTJs at higher bias. In our previous work,¹⁸ the double minima have been observed both in sputtered and electron beam evaporation grown SMTJs, which are usually attributed

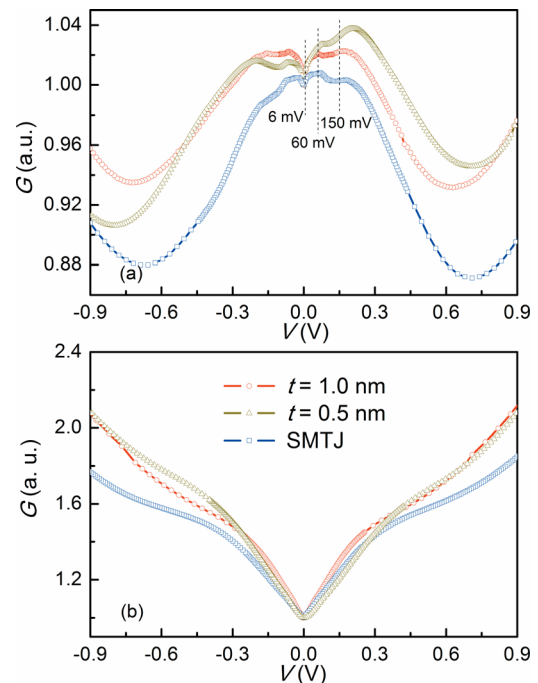


FIG. 3. (Color online) Dynamic conductance (dI/dV) for DMTJs and SMTJ in the parallel states (a) and antiparallel states (b). The bias axes in (a) and (b) are multiplied by 2 for the SMTJ.

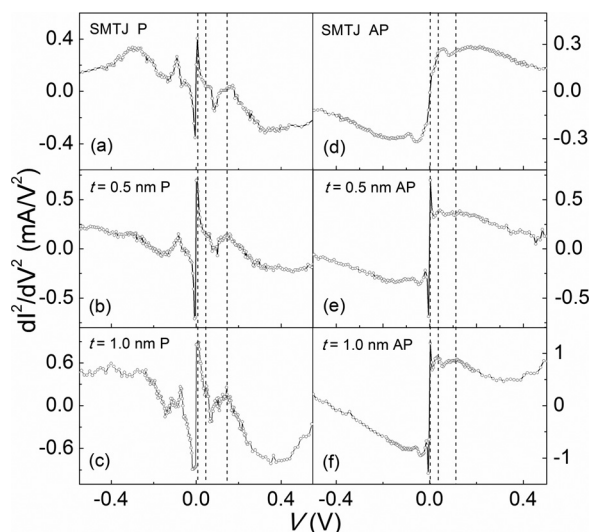


FIG. 4. IET spectra in the P [(a), (b) and (c)] and AP [(d), (e) and (f)] configurations at 2 K for the SMTJ and DMTJs.

to the contribution of the Δ_5 majority electron channel or Δ_1 minority electron channel.¹² Also, the double minima for DMTJs are quite similar to those of the scaled SMTJ. By comparing the dI/dV curves and IET spectra of the DMTJ and the scaled SMTJ, it appears that the tunneling mechanism in DMTJ is similar to that of two SMTJs in series.

The origins of the peaks in the IET spectra can be explained as follows: the zero-bias anomaly appearing at 6 mV (3 mV for the SMTJ) may be caused by magnetic impurities or electron-electron interactions in presence of disorder in CoFeB electrodes.^{12,13} A wide shoulder-like peak is located at around 60 mV (30 mV for the SMTJ) may be due to magnon excitation.^{12–16} Another wider peak visible around 150 mV (75 mV for SMTJ) is usually considered as a signature of MgO-phonon excitation.^{12–15} Thus, compared with the scaled SMTJ, all the features in dI/dV curve and peaks in IET spectra in DMTJs can be understood.

The dynamic conductance for the antiparallel configuration is shown in Fig. 3(b). No obvious features were observed as for the parallel state except the increase of conductance with bias. In the IET spectra for the antiparallel configuration, as shown in Figs. 4(d), 4(e), and 4(f), the positions of peaks for the scaled SMTJ and DMTJs are not coincident and the bias values of peak positions for DMTJs are smaller. It may be due to an ill-defined antiparallel state in the top MTJ, thus the bottom MTJ contributes more to the resistance and the IET spectra mainly reflects the bottom MTJ.

In our samples, no oscillation in conductance was observed at low temperature despite the high TMR. Possible reasons for the absence resonant tunneling in our DMTJs include the presence of boron in the free layer, relatively poor quality of top MgO compared to bottom MgO, and the absence of atomically flat surfaces over the entire junction area as pointed out by Herranz *et al.*⁸

IV. SUMMARY

In conclusion, we have investigated the dynamic conductance and IET spectra in SMTJ and DMTJs with a CoFe/CoFeB free layer. The CoFeB insertion can considerably improve the TMR ratio of the DMTJ. By comparing the DMTJs with a scaled SMTJ, the features in the dynamic conductance and IET spectra of the DMTJ were identified; it is suggested that DMTJ can be considered as two SMTJs in series. Unfortunately, no resonant tunneling could be observed in our devices, despite their high TMR.

ACKNOWLEDGMENTS

The project was supported by the State Key Project of Fundamental Research of Ministry of Science and Technology [MOST, No. 2010CB934400] and National Natural Science Foundation of China [NSFC, Grant No. 10934099, 10874225 and 51021061], and the partial support of K. C. Wong Education Foundation, Hong Kong. This work was also supported by the China-Ireland Joint Research Project between SFI and MOST, and by the SFI MANSE Project 05/IN/1850.

- ¹S. Yuasa, T. Nagahama, A. Fukushima, Y. Suzuki, and K. Ando, *Nat. Mater.* **3**, 868 (2004).
- ²S. S. P. Parkin, C. Kaiser, A. Panchula, P. M. Rice, B. Hughes, M. Samant, and S. H. Yang, *Nat. Mater.* **3**, 862 (2004).
- ³G. Feng, S. V. Dijken, and J. M. D. Coey, *Appl. Phys. Lett.* **89**, 162501 (2006).
- ⁴A. Reimartz, J. Schmalhorst, and G. Reiss, *J. Appl. Phys.* **105**, 014510 (2009).
- ⁵H. D. Gan, S. Ikeda, W. Shiga, J. Hayakawa, K. Miura, H. Yamamoto, H. Hasegawa, F. Matsukura, T. Ohkubo, K. Hono, and H. Ohno, *Appl. Phys. Lett.* **96**, 192507 (2010).
- ⁶G. Q. Yu, Z. Diao, J. F. Feng, H. Kurt, X. F. Han, and J. M. D. Coey, *Appl. Phys. Lett.* **98**, 112504 (2011).
- ⁷T. Nozaki, N. Tezuka, and K. Inomata, *Phys. Rev. Lett.* **96**, 027208 (2006).
- ⁸D. Herranz, F. G. Aliev, C. Tiusan, M. Hehn, V. K. Dugaev, and J. Barnas, *Phys. Rev. Lett.* **105**, 047207 (2010).
- ⁹G. X. Du, S. G. Wang, Q. L. Ma, Yan Wang, R. C. C. Ward, X. G. Zhang, C. Wang, A. Kohn, and X. F. Han, *Phys. Rev. B* **81**, 064438 (2010).
- ¹⁰Q. L. Ma, S. G. Wang, H. X. Wei, H. F. Liu, X.-G. Zhang, and X. F. Han, *Phys. Rev. B* **83**, 224430 (2011).
- ¹¹H. X. Wei, Q. H. Qin, Q. L. Ma, X. G. Zhang, and X. F. Han, *Phys. Rev. B* **82**, 134436 (2010).
- ¹²J. Bernos, M. Hehn, F. Montaigne, C. Tiusan, D. Lacour, M. Alnot, B. Negulescu, G. Lengaigne, E. Snoeck, and F. G. Aliev, *Phys. Rev. B* **82**, 060405(R) (2010).
- ¹³V. Drewello, M. Schäfers, O. Schebaum, A. A. Khan, J. Münchenberger, J. Schmalhorst, G. Reiss, and A. Thomas, *Phys. Rev. B* **79**, 174417 (2009).
- ¹⁴D. Bang, T. Nozaki, D. D. Djayaprawira, M. Shiraishi, Y. Suzuki, A. Fukushima, H. Kubota, T. Nagahama, S. Yuasa, H. Maehara, K. Tsunekawa, Y. Nagamine, N. Watanabe, and H. Itoh, *J. Appl. Phys.* **105**, 07C924 (2009).
- ¹⁵G. X. Miao, K. B. Chetry, A. Gupta, W. H. Butler, K. Tsunekawa, D. Djayaprawira, and G. Xiao, *J. Appl. Phys.* **99**, 08T305 (2006).
- ¹⁶K. Ono, T. Daibou, S. J. Ahn, Y. Sakuraba, T. Miyakoshi, T. Morita, Y. Kikuchi, M. Oogane, Y. Ando, and T. Miyazaki, *J. Appl. Phys.* **99**, 08A905 (2006).
- ¹⁷G. Feng, S. V. Dijken, and J. M. D. Coey, *J. Appl. Phys.* **105**, 07C926 (2009).
- ¹⁸H. Kurt, K. Oguz, T. Niizeki, and J. M. D. Coey, *J. Appl. Phys.* **107**, 083920 (2010).